2008

A novel control strategy for a variable speed wind turbine with a permanent magnet synchronous generator

M. E. Haque
University of Tasmania, mehaque@utas.edu.au

Michael Negnevitsky
University of Tasmania

Kashem Muttaqi
University of Wollongong, kashem@uow.edu.au

A Novel Control Strategy for a Variable Speed Wind Turbine with a Permanent Magnet Synchronous Generator

M. E. Haque, and M. Negnevitsky
Center for Renewable Energy and Power System
School of Engineering, University of Tasmania
Hobart, Australia
E-mail: mehaque@utas.edu.au

K. M. Muttaqi
School of Electrical, Computer and Telecommunication
Engineering, University of Wollongong
Wollongong, Australia

Abstract— **This paper presents a novel control strategy for the operation of a direct drive permanent magnet synchronous generator (PMSG) based stand alone variable speed wind turbine. The control strategy for the generator side converter with maximum power extraction is discussed. The stand alone control is featured with output voltage and frequency controller capable of handling variable load. The potential excess of power is dissipated in the damp resistor with the chopper control and the dc link voltage is maintained. Dynamic representation of dc bus and small signal analysis are presented. Simulation results show that the controllers can extract maximum power and regulate the voltage and frequency under varying wind and load conditions. The controller shows very good dynamic and steady state performance.**

Keywords- Permanent magnet synchronous generator, maximum power extraction, switch-mode rectifier, variable speed wind turbine, voltage and frequency control.

I. INTRODUCTION

Variable speed wind turbines have many advantages over fixed speed generation such as increased energy capture, operation at maximum power point, improved efficiency and power quality [1]. However, the presence of gearbox that couples the wind turbine to the generator causes problems. The gearbox suffers from faults and requires regular maintenance [2]. The reliability of the variable speed wind turbine can be improved significantly by using a direct drive permanent magnet synchronous generator. PMSG has received much attention in wind energy application because of their property of self excitation, which allows an operation at a high power factor and high efficiency [3]. The use of permanent magnet in the rotor of the PMSG makes it unnecessary to supply magnetizing current through the stator for constant air- gap flux; the stator current need only to be torque producing. Hence for the same output, the PMSG will operate at a higher power factor because of the absence of the magnetizing current and will be more efficient than other machines.

To extract maximum power from the fluctuating wind, variable speed operation of the wind turbine generator is necessary. This requires a sophisticated control strategy for the generator. Optimum power/torque tracking is popular control strategy as it helps to achieve optimum wind energy utilization [4-8]. Some of these control strategies use wind velocity to obtain the desired shaft speed to vary the generator speed. However, anemometer based control strategy increases cost and reduce the reliability of the overall system. These control strategies are not suitable or too expensive for a small scale wind turbine. In [7], the current vector of an interior type PMSG is controlled to optimize the wind turbine operation at various wind speed, which requires six active switches to be controlled. Switch-mode rectifier has been investigated for use with automotive alternator with permanent magnet synchronous machines [9,10]. The switch-mode rectifier has also been investigated for small scale variable speed wind turbine [11, 12].

A control strategy for the generator side converter with output maximization of a PMSG based small scale wind turbine is developed. The generator side switch mode rectifier is controlled to achieve maximum power from the wind. The method requires only one active switching device (IGBT), which is used to control the generator torque to extract maximum power. It is simple and a low cost solution for a small scale wind turbine.

For a stand alone system, the output voltage of the load side converter has to be controlled in terms of amplitude and frequency. Previous publications related to PMSG based variable speed wind turbine are mostly concentrated on grid connected system [6-8]. Much attention has not been paid for a stand alone system. Many countries are affluent in renewable energy resources; however they are located in remote areas where power grid is not available. Local, small scale stand-alone distributed generation system that can utilize these renewable energy resources when grid connection is not feasible. In this paper, a control strategy is developed to control the load voltage in a stand alone mode. As there is no grid in a stand-alone system, the output voltage has to be controlled in terms of amplitude and frequency. The load side PWM (pulse width modulation) inverter is using a relatively complex vector control scheme to control the amplitude and frequency of the inverter output voltage. The stand alone control is featured with output voltage and frequency controller capable of handling variable load. A damp resistor controller is used to dissipate excess power during fault or over-generation. The excess power is dissipated in the damp resistor with the chopper control and the dc link voltage is maintained.

978-1-4244-2279-1/08/$25.00 © 2008 IEEE

II. WIND TURBINE CHARACTERISTICS

The amount of power captured by the wind turbine (power delivered by the rotor) is given by

$$P_t = 0.5\rho A C_p(\lambda,\beta)\times(v_w)^3 = 0.5\rho A C_p \times \left(\frac{\omega_m R}{\lambda}\right)^3 \quad (1)$$

Where, ρ is the air density (kg/m^3), v_ω is the wind speed in m/s, A is the blades swept area, C_p is the turbine rotor power coefficient, which is a function of tips peed ratio (λ) and pitch angle (β). ω_m = rotational speed of turbine rotor in mechanical rad/s, and R = radius of the turbine. The coefficient of performance of a wind turbine is influenced by the tip-speed to wind speed ratio, which is given by,

$$TSR = \lambda = \frac{\omega_m R}{v_w} \quad (2)$$

The wind turbine can produce maximum power when the turbine operates at maximum C_p (i.e. at C_{p_opt}). So it is necessary to keep the rotor speed at an optimum value of the tip speed ratio, λ_{opt} . If the wind speed varies, the rotor speed should be adjusted to follow the change.

The target optimum power from a wind turbine can be written as,

$$P_{m\_opt} = 0.5\rho A C_{p\_opt}\left(\frac{\omega_{m\_opt} R}{\lambda_{opt}}\right)^3 = K_{opt}\left(\omega_{m\_opt}\right)^3 \quad (3)$$

Where, $K_{opt} = 0.5\rho\ A\ C_{p\_opt}\left(\frac{R}{\lambda_{opt}}\right)^3$ (4)

and $\omega_{m\_opt} = \frac{\lambda_{opt}}{R} v_w = K_w v_w$ (5)

Therefore, the target optimum torque can be given by

$$T_{m\_opt} = K_{opt}\left(\omega_{m\_opt}\right)^2 \quad (6)$$

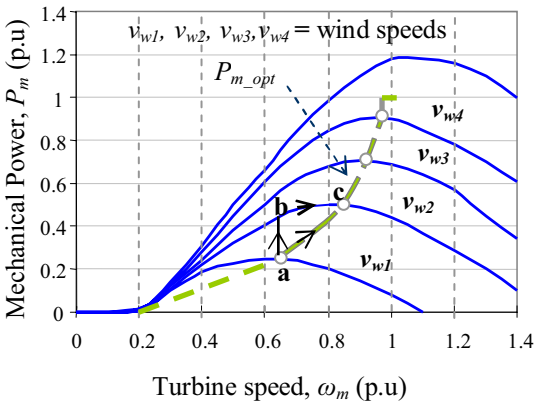

Figure 1. Mechanical power generated by turbine as a function of the rotor speed for different wind speed.

The mechanical rotor power generated by turbine as a function of the rotor speed for different wind speed is shown in fig. 1. The optimum power is also shown in this figure. The optimum power curve (P_{opt}) shows how maximum energy can be captured from the fluctuating wind. The function of the controller is to keep the operating of the turbine on this curve, as the wind velocity varies. It is observed from this figure that there is always a matching rotor speed which produces maximum power for any wind speed. If the controller can properly follow the optimum curve, the wind turbine will produce maximum power at any speed within the allowable range. The optimum torque can be calculated from the optimum power given by (6). For the generator speed below the rated maximum speed, the generator follows (6).

III. SYSTEM OVERVIEW

Fig. 2 shows the control structure of a PMSG based standalone variable speed wind turbine which include a wind turbine, PMSG, single switch three phase switch-mode rectifier and a vector controlled PWM voltage source inverter.

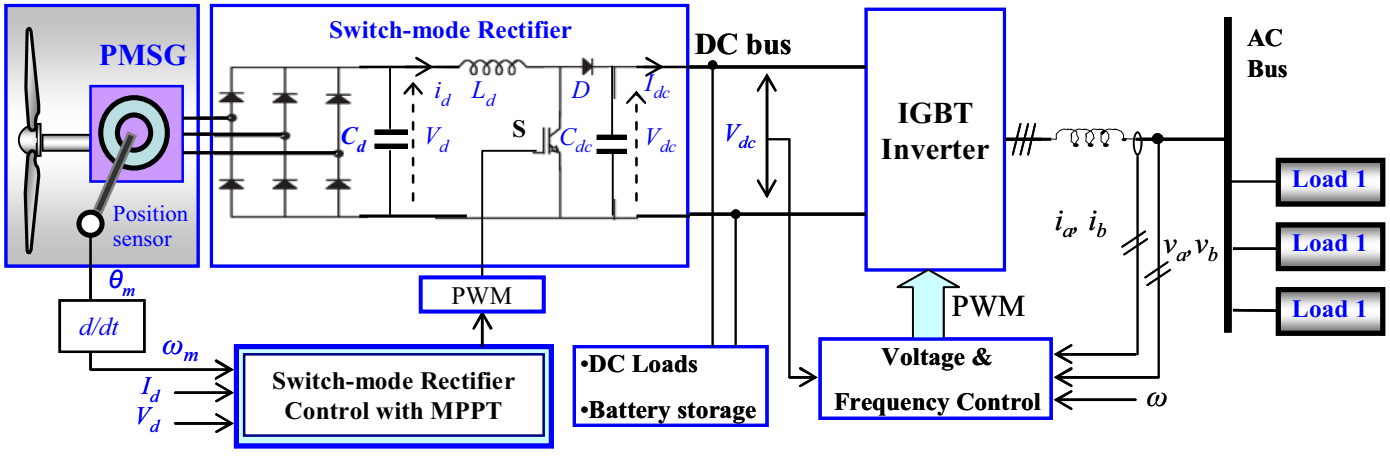

Figure 2. Control Structure of a PMSG based standalone variable speed wind turbine.

The output of a variable speed PMSG is not suitable for use as it varies in amplitude and frequency due to fluctuating wind. A constant DC voltage is required for direct use, storage or conversion to AC via an inverter. In this paper, a single switch three-phase switch-mode rectifier is used to convert the ac output voltage of the generator to a constant dc voltage before conversion to AC voltage via an inverter.

The single switch three phase switch-mode rectifier consists of a three-phase diode bridge rectifier and a DC to DC converter. The output of the switch-mode rectifier can be controlled by controlling the duty cycle of an active switch (such as IGBT) at any wind speed to extract maximum power from the wind turbine and to supply the loads.

IV. CONTROL OF SWITCH-MODE RECTIFIER WITH MAXIMUM POWER EXTRACTION

The structure of the proposed control strategy of the switch mode rectifier is shown in fig. 3. The control objective is to control the duty cycle of the switch ***S*** in fig. 2, to extract maximum power from the variable speed wind turbine and transfer the power to the load. The control algorithm includes the following steps:

- Measure generator speed, ω_g.
- Determine the reference torque (fig. 4) using the following equation:

$$T_g^* = K_{opt}(\omega_g)^2 \tag{7}$$

- This torque reference is then used to calculate the DC current reference by measuring the rectifier output voltage, V_d as given by:

$$I_d^* = (T_g^* \times \omega_g)/V_d \tag{8}$$

- The error between the reference dc current (and measured dc current is used to vary the duty cycle of the switch to regulate the output of the switch-mode rectifier and the generator torque through a PI controller.

The generator torque is controlled in the optimum torque curve in fig. 4 according to generator speed. The acceleration or deceleration of the generator is determined by the difference of the turbine torque T_m and generator torque T_g. If the generator speed is less than the optimal speed, the turbine torque is larger than the generator torque and the generator will be accelerated. The generator will be decelerated if the generator speed is higher than the optimal speed. Therefore, the turbine torque and generator torque settle down to the optimum torque point T_{m_opt} at any wind speed and the wind turbine is operated at the maximum power point. For example (considering fig. 1), if the PMSG operating at point '**a**' and wind speed increases from v_{w1} to v_{w2} (point '**b**'), the additional power and hence torque causes the PMSG to accelerate. The accelerating torque is the difference between the turbine mechanical torque and the torque given by the optimum curve. Finally, the generator will reach the point '**c**' where the accelerating torque is zero. A similar situation occurs when the wind velocity decreases.

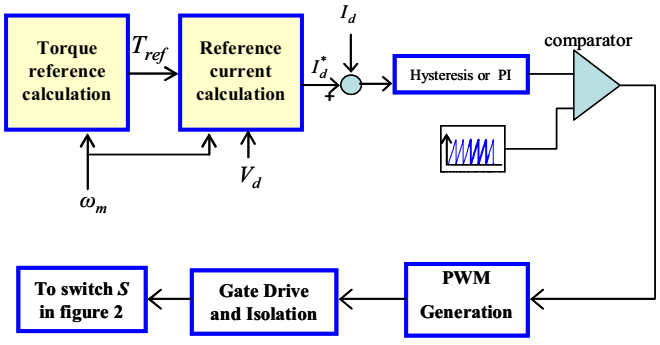

Figure 3. Control strategy of the switch-mode rectifier.

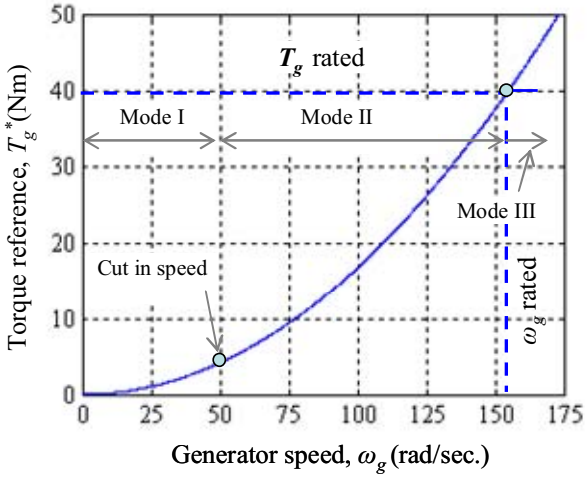

Figure 4. Generator torque reference versus speed.

In the proposed method, the wind speed is not required to be monitored and therefore, it is a simple output maximization control method without wind speed sensor (anemometer).

V. CONTROL OF LOAD SIDE INVETER

The objective of the supply side converter is to regulate the voltage and frequency. The output voltages have to be controlled in terms of amplitude and frequency as there is no grid exists in a stand-alone system. The control structure for stand-alone control mode is consists of output voltage controller, dc link voltage controller, damping resistance controller and current controller. The Output voltage controller is used to control the output voltage during load transients or wind variation. DC-link voltage controller is used to stabilize the dc link voltage. The dc-voltage PI controller maintains the dc voltage to the reference value. PI controllers are used to regulate the output voltage and currents in the inner control loops and the dc voltage controller in the outer loop. To compensate the cross-coupling effect due to the output filter in the rotating reference frame, compensation terms are added as shown in fig. 5. All the PI controllers are tuned using Ziegler-Nichols tuning method [13].

The vector control scheme used is based on a synchronously rotating reference frame as shown in figure 6. The angular velocity of the rotating axis system ω is set in the controller and defines the electrical frequency at the load. The voltage balance across the inductor L_f is given by

$$\begin{bmatrix} v_a \\ v_b \\ v_c \end{bmatrix} = R_f \begin{bmatrix} i_a \\ i_b \\ i_c \end{bmatrix} + L_f \frac{d}{dt} \begin{bmatrix} i_a \\ i_b \\ i_c \end{bmatrix} + \begin{bmatrix} v_{a1} \\ v_{b1} \\ v_{c1} \end{bmatrix} \quad (9)$$

Where, L_f and R_f are the filter inductance and resistance respectively. v_{a1}, v_{b1}, v_{c1} represent voltages at the inverter output. i_a, i_b and i_c are the line currents.

The vector representation of a balanced three phase system and their equivalent vectors in a rotating dq reference frame is shown in fig. 6. Transforming the voltage equations using *dq* transformation in the rotating reference frame:

$$v_d = v_{di} - R_f i_d - L_f \frac{di_d}{dt} + \omega L_f i_q \quad (10)$$

$$v_q = v_{qi} - R_f i_q - L_f \frac{di_q}{dt} - \omega L_f i_d \quad (11)$$

The instantaneous power in a three phase system is given by:

$$P(t) = v_a i_a + v_b i_b + v_c i_c = [v_a \quad v_b \quad v_c][i_a \quad i_b \quad i_c]' \quad (12)$$

Using *dq* transformation, the active and reactive power is given by

$$P = \frac{3}{2}(v_d i_d + v_q i_q) \quad (13)$$

$$Q = \frac{3}{2}(v_d i_q + v_q i_d) \quad (14)$$

If the reference frame is as $v_q = 0$ and $v_d = |V|$, the equations for active and reactive power will be,

$$P = \frac{3}{2}(v_d i_d) = \frac{3}{2}|V| i_d \quad (15)$$

$$Q = \frac{3}{2}(v_d i_q) = \frac{3}{2}|V| i_q \quad (16)$$

Therefore, active and reactive power can be controlled by controlling direct and quadrature current components, respectively.

VI. DC BUS DYNAMICS AND PROTECTION

A damp resistor controller is used to dissipate excess power during fault or over-generation. The potential excess of power will be dissipated in the damp resistor with the chopper control and the dc link voltage will be maintained. The control is linear and increase the duty cycle as a function of the over voltage amount. If the dc link voltage exceeds the maximum limit, the DC link will be short circuited through the resistor R_D as shown in fig. 7. Using the power balance principle, the dynamic behaviour of the dc bus voltage V_{dc} is given by

$$\frac{d\left(\frac{1}{2}CV_{dc}^2\right)}{dt} = P_G - \frac{V_{dc}^2}{R_D} - P_{IN} \quad (17)$$

$$\Rightarrow \frac{d(V_{DC}^2)}{dt} = \frac{2}{C} \times \left(P_G - \frac{V_{dc}^2}{R_D} - P_{IN} \right)$$

$$\Rightarrow V_{dc} = \sqrt{\frac{2}{C} \int \left(P_G - \frac{V_{dc}^2}{R_D} - P_{IN} \right) dt} \quad (18)$$

Where P_G = Power from the generator, $\frac{V_{dc}^2}{R_D}$ = power dissipated in the damp load resistor (R_D), and P_{IN} = power at the input of the inverter.

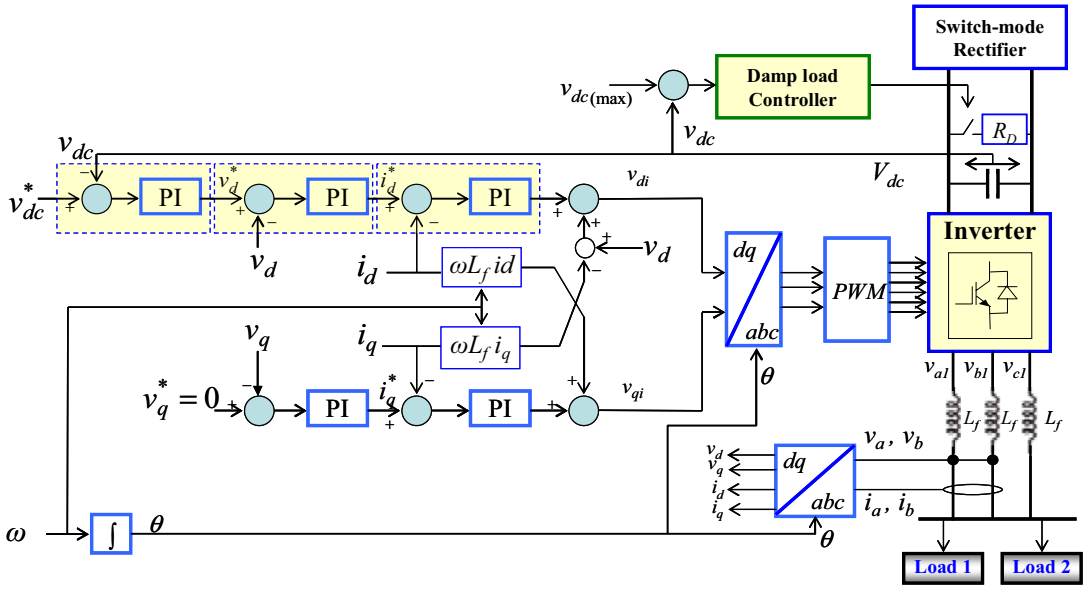

Figure 5. Vector control structure for stand alone mode of operation

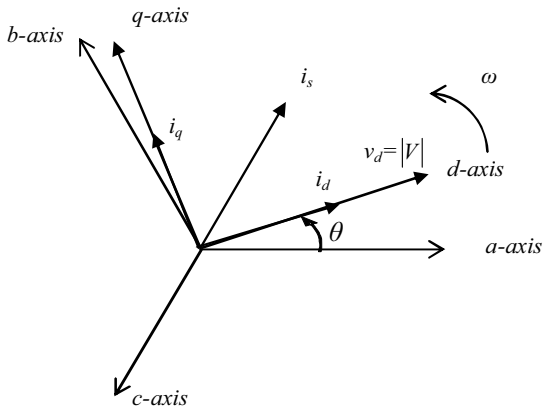

Figure 6. abc and rotating reference frame.

VII. Small Signal Analysis

Considering the load power factor close to unity, the reactive power supplied by the converter will be negligible. So the quadrature component of the load current will be zero. For a R_L load, the *d-q* equations for the load side of the fig. 7(a) are,

$$I_{IN} \approx \frac{v_d i_{dL}}{V_{dc}} \tag{19}$$

$$v_d = i_{dL} R_L \tag{20}$$

Where v_d and i_{dL} are the direct component of the load voltage and current, respectively.

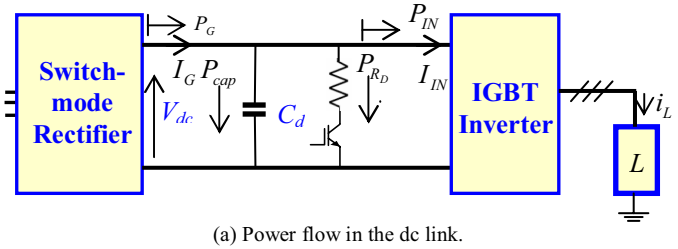

(a) Power flow in the dc link.

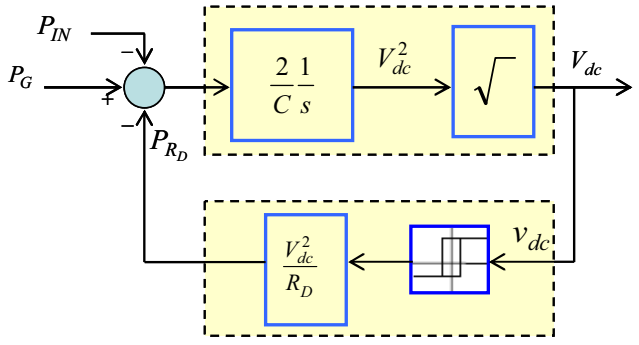

(b) DC bus dynamics and protection.

Figure 7. Dynamic representation of DC bus and protection.

The dc link voltage V_{dc} is given by

$$V_{dc} = \frac{I_G - I_{IN}}{sC_{dc}} \tag{21}$$

Where C_{dc} is the dc link capacitance. Using (19-21), the block diagram of fig. 8(a) can be obtained. In fig. 8(a), $G_{dc}(s)$ is the dc-link voltage controller as shown in fig. 5 and $G_{ac}(s)$ is the controller of the ac load voltage. The control system of fig. 8(a) is non linear with coupling between the dc-link voltage control loop and load voltage control loop. Linearizing around a quiescent point $(V_{dc0}, v_{d0}, i_{dL0}, I_{G0}, I_{IN0})$ gives,

$$\Delta I_{IN} = \frac{\Delta v_d i_{dL0} + \Delta i_{dL} v_{d0}}{V_{dc0}} - \frac{v_{d0} i_{dL0}}{V_{dc0}^2} \Delta V_{dc} \tag{22}$$

$$\Delta V_{dc} = \frac{\Delta I_G - \Delta I_{IN}}{sC_{dc}} \tag{23}$$

Under normal operation, the small signal model can be simplified by considering that the variation in dc link voltage and direct axis component of the load voltage are small compared to the variation in load currents. Therefore,

$$\frac{v_{d0}}{V_{dc0}} \Delta i_{dL} \rangle\rangle \frac{i_{dL0}}{V_{dc0}} \Delta v_d - \frac{v_{d0} i_{dG0}}{V_{dc0}^2} \Delta V_{dc} \tag{24}$$

Using (22-24), the small signal model of fig. 8(b) is obtained. There is still some coupling between dc link voltage and the load voltage control loops in fig. 8(b). However, because of the high inertia of the wind turbine [14], the current will vary slowly compared with the natural frequency of the load voltage control loop. Therefore, the load voltage can be considered almost constant for the dc link voltage control loop and the open loop transfer function $\frac{\Delta V_{dc}}{\Delta i_{dL}}$ is obtained as,

$$\frac{\Delta V_{dc}}{\Delta i_{dL}} \approx \frac{v_{d0}}{sC_{dc} V_{dc}^*} \tag{25}$$

A PI controller can be designed using (25). The open loop transfer function for the load voltage control loop can also be obtained from fig. 8(b) as,

$$\frac{\Delta v_d}{\Delta i_{dL}} \approx R_L \tag{26}$$

Considering the output filter capacitance (C_f) and neglecting the cross coupling between the d and q axes, the open loop transfer function $\frac{\Delta v_d}{\Delta i_{dL}}$ is given by,

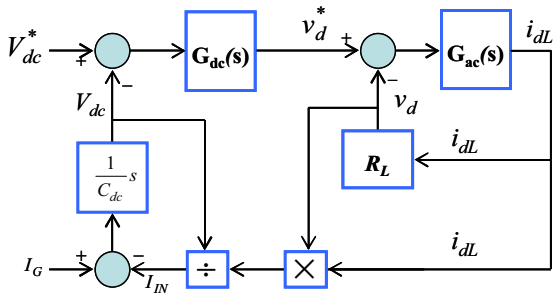

(a) Control system.

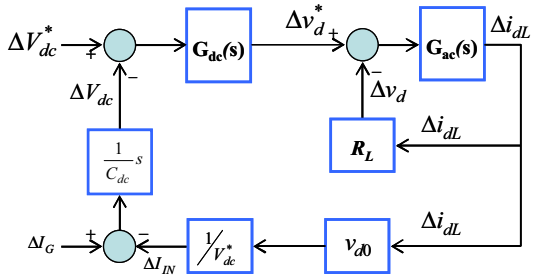

(b) Small signal model.

Figure 8. Block diagram of the proposed control system.

$$\frac{\Delta v_d}{\Delta i_{dL}} \approx \frac{R_L}{1+sR_LC_f} \tag{27}$$

Using (27), a PI controller for load voltage control loop can be designed. The transfer function of (27) is obtained considering a resistive load. For a $R_L - L$ load, the transfer function of the filter capacitance and the load can be obtained (neglecting cross coupling terms) as,

$$\begin{bmatrix} v_d \\ v_q \end{bmatrix} \approx \frac{(s+R_L/L)}{C_f(s^2+(R_L/L)s+1/(LC_f))} \begin{bmatrix} i_{dL} \\ i_{qL} \end{bmatrix} \tag{28}$$

Where v_d, v_q are the *d*-*q* axes components of the load voltage.

VIII. RESULTS AND DISCUSSION

The model of the PMSG based variable speed wind turbine system of fig. 2 is built using Matlab/Simpower dynamic system simulation software. The simulation model is developed based on a Kollmorgen 6 kW industrial permanent magnet synchronous machine. The parameters of the Turbine and PMSG used are given in Table I. The power converter and the control algorithm are also implemented and included in the model. The sampling time used for the simulation is 20 µs.

Fig. 9 shows the response of the system for a step change of wind speed from 10 m/s to 12 m/s to 9 m/s and then comes back to 10 m/s. It is seen from fig. 9 (c) that the generated torque reference follows the optimum mechanical torque of the turbine quite well. The generator electromagnetic torque also track the reference torque as shown in fig. 9(d).

Fig. 9(e) shows the reference dc current and measured DC current. It is observed that the measured DC current follows the reference DC current and regulate the turbine torque to extract maximum power from the wind turbine. Fig. 9(f) dc output power.

Fig. 10 shows optimum torque versus speed as well as generator torque versus speed. Turbine mechanical input power and electrical output powers are shown in fig. 11. It is observed that the torque and power follow the optimum curves up to the rated speed and extract maximum power.

The simulation results demonstrate that the controller works very well and shows very good dynamic and steady state performance. The control algorithm can be used to extract maximum power from the variable speed wind turbine under fluctuating wind.

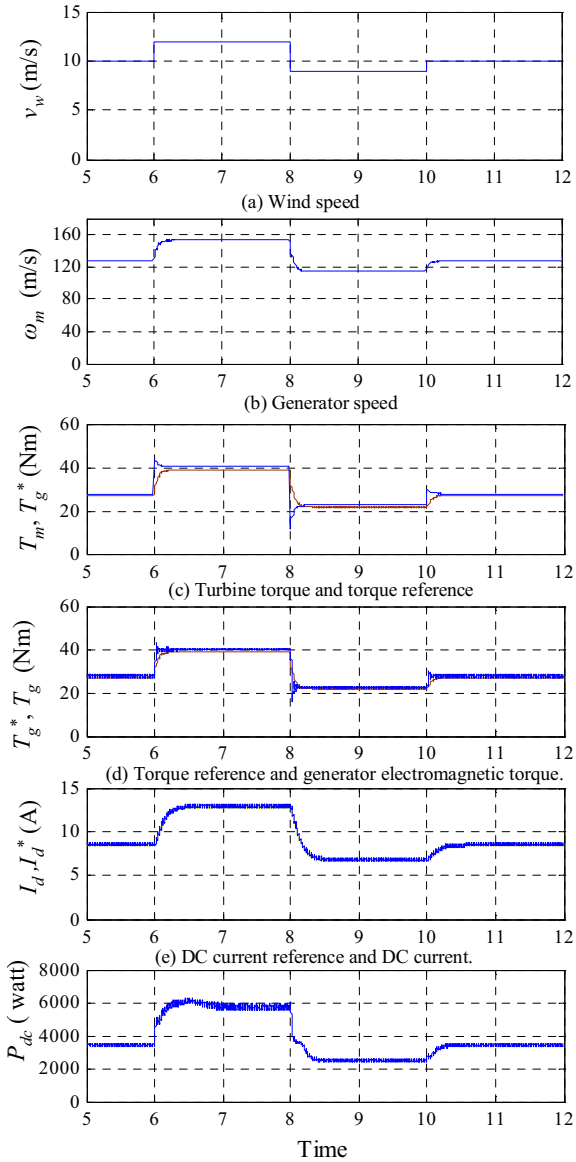

Figure 9. Response of the system for a step change of wind speed from 10 m/s to 12 m/s to 9 m/s to 10 m/s.

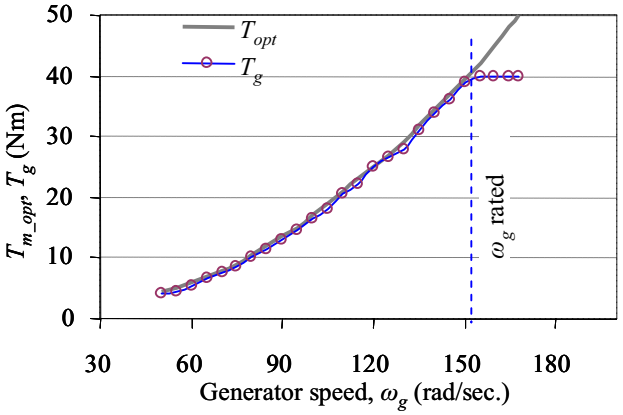

Figure 10. Optimum torque and generator torque.

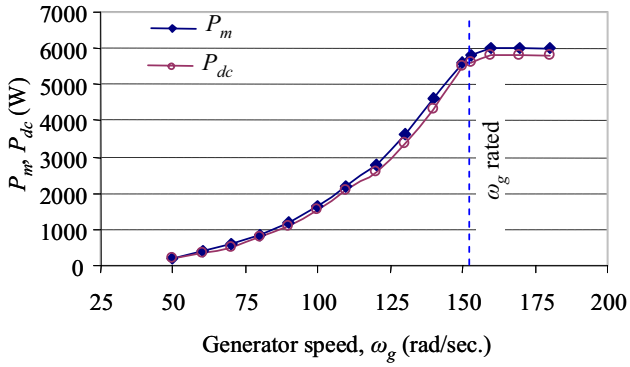

Figure 11. Turbine mechanical input power and Electrical output power.

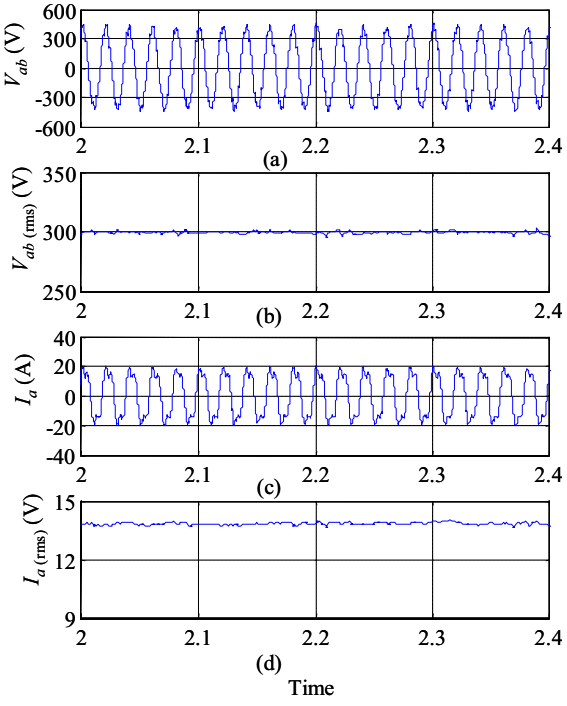

Figure 12. Voltage and current responses at a constant load.

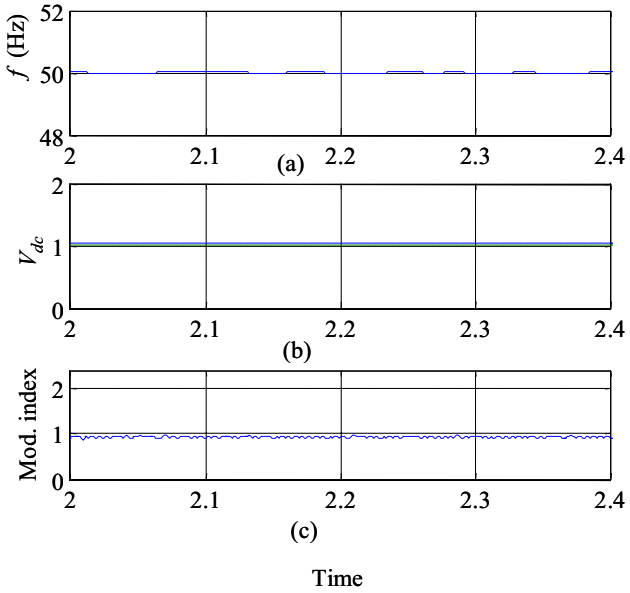

Figure 13. Frequency response, DC link voltage and modulation index at a constant load.

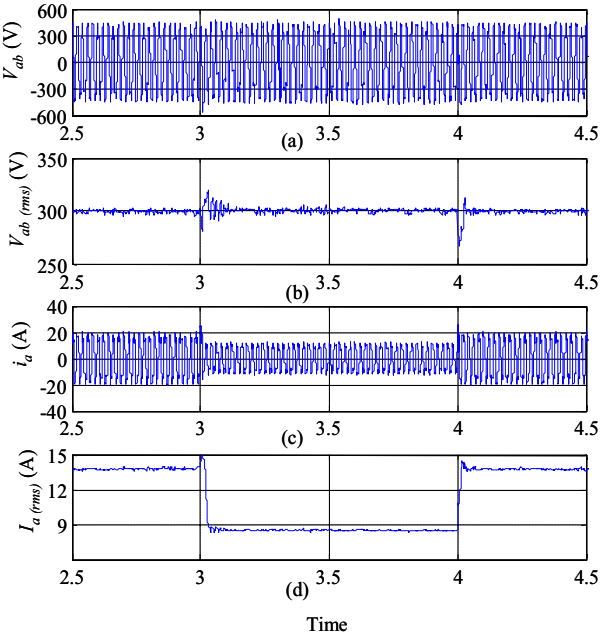

Figure 14. Voltage and current responses when load is reduced by 50%.

Fig. 12 shows the load voltage and current responses. Fig. 12(a) and 12(b) show instantaneous and rms load voltages and figure 12(c) and 12(d) show instantaneous and rms currents at a constant load. Fig. 13 shows the frequency response, dc link voltage and modulation index of the PWM inverter at a constant load.

Fig. 14 shows the load voltage, current and fig. 15 shows the frequency response, dc link voltage and modulation index of the PWM inverter when the load is reduced to 50%

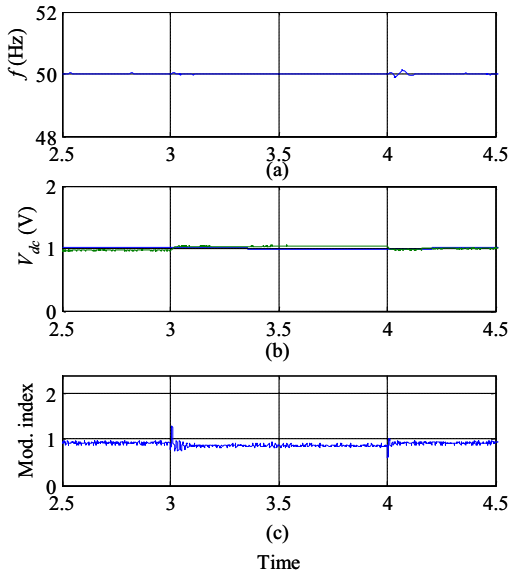

Figure 15. Frequency response, DC link voltage and modulation index when load is reduced by 50%.

during $3s \le t \le 4s$. Fig. 14(a) and 14(b) show instantaneous and rms voltages and fig. 14(c) and 14(d) show the instantaneous and rms currents when the load is reduced to 50% at $t = 3s$ and remains at this value until $t = 4s$. Fig. 15 shows the corresponding frequency response, dc link voltage and modulation index. It is seen that the controller can regulate the load voltage and frequency quite well at constant load and under varying load condition.

IX. CONCLUSIONS

Control strategy for a direct drive stand alone variable speed wind turbine with a PMSG is presented in this paper. A simple control strategy for the generator side converter to extract maximum power is discussed and implemented using Simpower dynamic system simulation software. The controller is capable to maximize output of the variable speed wind turbine under fluctuating wind. The load side PWM inverter is controlled using vector control scheme to maintain the amplitude and frequency of the inverter out put voltage. It is seen that the controller can maintain the load voltage and frequency quite well at constant load and under varying load condition. The generating system with the proposed control strategy is suitable for a small scale standalone variable speed wind turbine installation for remote area power supply. The simulation results demonstrate that the controller works very well and shows very good dynamic and steady state performance.

ACKNOWLEDGMENT

This work is supported by the Australian research Council ARC) and Hydro Tasmania Linkage Grant, K0015166. The authors greatly acknowledge the support and cooperation of hydro Tasmania personnel in providing data and advice on the operation of remote area power supply system.

TABLE I: PARAMETERS OF TURBINE-GENERATOR SYSTEM

Wind turbine	
Density of air	1.225 Kg/m^3
Area swept by blades, A	1.06 m^2
Optimum coefficient, K_{opt}	1.67×10^{-3} Nm/(rad/s)^2
Base wind speed	12 m/s
PMSG	
No. of poles	10
Rated speed	153 rad/sec
Rated current	12 A
Armature resistance, R_s	0.425 Ω
Magnet flux linkage	0.433 Wb
Stator inductance, L_s	8.4 mH
Rated torque	40 Nm
Rated power	6 KW

REFERENCES

[1] Müller, S., Deicke, M., and De Doncker, Rik W.: 'Doubly fed induction genertaor system for wind turbines', IEEE Industry Applications Magazine, May/June, 2002, pp. 26-33.

[2] Polinder H., Van der Pijl F. F. A, de Vilder G. J., Tavner P. J.: "Comparison of direct-drive and geared generator concepts for wind turbines," IEEE Trans. on energy conversion, 2006, . 21, (3), pp. 725-733.

[3] Chan T. F., and Lai L. L., "Permanenet-magnet machines for distributed generation: a review," Proc. IEEE power engineering annual meeting, 2007, pp. 1-6.

[4] De Broe M., Drouilhet S., and Gevorgian V.: "A peak power tracker for small wind turbines in battery charging applications," *IEEE Trans. Energy Convers.* 1999, 14, (4), pp. 1630–1635.

[5] Datta R., and Ranganathan V. T.: "A method of tracking the peak power points for a variable speed wind energy conversion system," IEEE Trans. Energy Convers., 1999, 18, (1), pp. 163–168.

[6] Tan K., and Islam S.: "Optimal control strategies in energy conversion of PMSG wind turbine system without mechanical sensors," IEEE Trans. Energy Convers., 2004, 19, (2), pp. 392–399.

[7] . Morimoto S, Nakayama H., Sanada M., and Takeda Y.: "Sensorless Output Maximization Control for Variable-Speed Wind Generation System Using IPMSG", IEEE Trans. Ind. Appl., 2005, 41, (1), pp. 60-67.

[8] Chinchilla M., Arnaltes S., and. Burgos J. C.: "Control of Permanent-Magnet Generators Applied to Variable-Speed Wind-Energy Systems Connected to the Grid" IEEE Trans. on Energy Conver., 2006, 21, (1), pp. 130-135.

[9] Perreault D.J., and Caliskan V.: "Automotive Power Generation and Control", IEEE Transactions on Power Electronics, 2004, 19, (3), pp. 618-630.

[10] Soong W.L., and Ertugrul N.: "Inverterless high-power interior permanent-magnet automotive alternator", IEEE Transactions on Industry Applications, 2004, 40, (4), pp.1083-1091.

[11] Whaley D. M., Soong W. L., Ertugrul N.: "Investigation of switched-mode rectifier for control of small-scale wind turbines", in proc. IEEE Industry Applications Society Annual Meeting, 2005, pp. 2849-2856.

[12] Muljadi E., Drouilhet S., Holz, R., and Gevorgian V.: "Analysis of permanent magnet genertaor for wind power battery charging", in proc. IEEE Industry applications society annual meeting, 1996, pp. 541-548.

[14] Astrom K. J,. and T. Hagglund,: "PID controllers: Theory, Design and Tuning", Research Triangle Park, NC: Instrument Society of America, 1995.

[15] A. Miller, Muljadi E., and Zinger D.: "A variable Speed Wind Turbine Power Control" IEEE Trans. on Energy Conversion, 1997, 12, (2), pp. 181-186.